Paper:

Development of Building Inventory Data and Earthquake Damage Estimation in Lima, Peru for Future Earthquakes

Masashi Matsuoka[*1], **Shun Mito**[*2], **Saburoh Midorikawa**[*1], **Hiroyuki Miura**[*3], **Luis G. Quiroz**[*4], **Yoshihisa Maruyama**[*4], **and Miguel Estrada**[*5]

[*1]Interdisciplinary Graduate School of Science and Engineering, Tokyo Institute of Technology
Nagatsuta 4259-G3, Midori-ku, Yokohama 226-8502, Japan
E-mail: matsuoka.m.ab@m.titech.ac.jp
[*2]Mitsubishi Jisho Property Management Co., Ltd., Tokyo, Japan
[*3]Graduate School of Engineering, Hiroshima University, Hiroshima, Japan
[*4]Graduate School of Engineering, Chiba University, Chiba, Japan
[*5]Japan-Peru Center for Earthquake Engineering and Disaster Mitigation (CISMID),
National University of Engineering, Lima, Peru
[Received August 6, 2014; accepted September 1, 2014]

Even though detailed building inventory data are necessary for estimating earthquake damage reliably, most developing countries do not have sufficient data for such estimations. This necessitates a way for finding building distribution and feature easily. In this study for estimating the number of households in all building categories of different structures or floor numbers in Lima, Peru, where a great earthquake is expected, we propose an estimation method based on existing GIS data from a census, satellite imagery, and building data from field surveys, and apply it to estimate the entire area of Lima for create building inventory data. Building fragility functions were used to calculate a severe damage ratio of buildings due to the expected earthquake. The rate was multiplied by created building inventory data to estimate the number of households in damaged buildings. Furthermore we clarified damage reduction by retrofitting for low earthquake-resistant buildings.

Keywords: building inventory data, earthquake damage estimation, census data, fragility curve, socio-economic class, satellite imagery

1. Introduction

Estimating earthquake damage to a variety of different building structures plays an important role in seismic disaster prevention planning. In estimating earthquake damage, damage distribution of buildings is estimated by multiplying building inventory data by damage probability obtained from the seismic capacity of buildings and earthquake ground motion. The estimation flow is shown in **Fig. 1**. Estimating earthquake damage thus requires earthquake ground motion data, the fragility curves of buildings, and building inventory data.

Building inventory data are usually created by visually analyzing aerial photography and field surveys, but this requires significant labor and cost. Developing countries rarely have sufficient building inventory data, which also makes it difficult to estimate earthquake damage appropriately. As in Japan, Peru is located close to a continental plate boundary where a seafloor plate sinks in a nearby ocean trench. Peru thus has frequent great earthquakes and must be able to estimate earthquake damage to determine effective disaster prevention and reduction countermeasures, even though Peru does not have enough building inventory data.

Estimating earthquake damage requires building inventory features such as construction type and the number of stories. Building deformation resistance and seismic capacity depend both on the construction type and whether the building is high-rise or low-rise. The number of stories thus becomes important to estimation.

Construction data can be collected integratedly and comprehensively from census data and establishment statistics. Hasegawa and Midorikawa (1997) and (1999) proposed estimating the distribution of wooden and non-wooden buildings and building age by using regional grid-square statistics [1, 2].

Remote sensing technology has steadily improved and satellite images with a ground resolution of 1m or less is now available. We can obtain height information for buildings. In developing building inventory data on Metropolitan Manila, for example, Miura and Midorikawa (2006) used IKONOS satellite images to automatically detect mid- and high-rise buildings from image shadows and to update existing building inventory data [3]. Shaker et al. (2011) used stereo pair images from IKONOS satellite that observed dense residential area in Cairo, Egypt, to estimate building height [4]. For Lima, Peru, building height was estimated by filtering digital surface model (DSM) of PRISM images from ALOS satellite [5].

In the present study, we proposed simple estimation method to the number of households in buildings in order

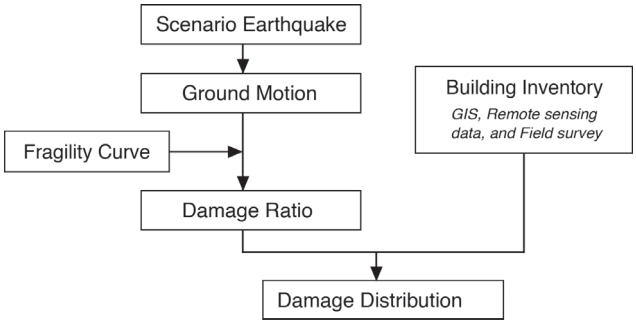

Fig. 1. Flowchart of earthquake damage estimation for large area.

to create necessary inventory data for estimating earthquake damage in Peru. For this purpose, we used Peru census data, field survey data, and satellite imagery to classify buildings by construction type and floor number for use in damage estimation. This method was used to develop building inventory data for all of Lima. This study also estimates building damage in Lima that an expected earthquake could cause and examines the damage reduction hoped for through earthquake retrofit for low earthquake-resistant buildings.

2. Target Area and Data

2.1. Target Area

Peru is located near the boundary between the South American and Nasca tectonic plates, making it the site of many earthquakes, e.g., the 2001 Southern Peru earthquake and the 2007 Pisco earthquake. Public concern about earthquake disaster prevention is understandably high in Peru. A great earthquake is expected to occur in and around Peru's capital Lima and earthquake disaster prevention countermeasures must be taken as soon as possible.

Target areas in Lima for this study are shown in **Fig. 2**. Lima consists of 50 districts and has an area of 2,700 km^2 and a population of about 8 million. It is one of the largest business and industrial cities in South America.

2.2. Census and Building Feature Data

One of the Peru's GIS data, including building information, is census on Lima [6]. This GIS data collected by the Peru Statistics Agency in 2007 covered most of Lima's 75,000 city blocks. The number of households and 5 levels of socioeconomic class in each block are listed with data on residential type, wall-construction, etc. Residential types are individual housing and collective housing, e.g., hotels and hospitals. Since 99.8% of residents lived in individual houses, we used individual housing data classified by detached house, apartment building, cooperative dwelling with independent kitchen and bathroom (quinta), and cooperative dwelling with shared kitchen and bathroom (callejón).

The distribution of detached houses, apartment buildings, and quinta are shown in **Figs. 3(a)–(c)**. Detached

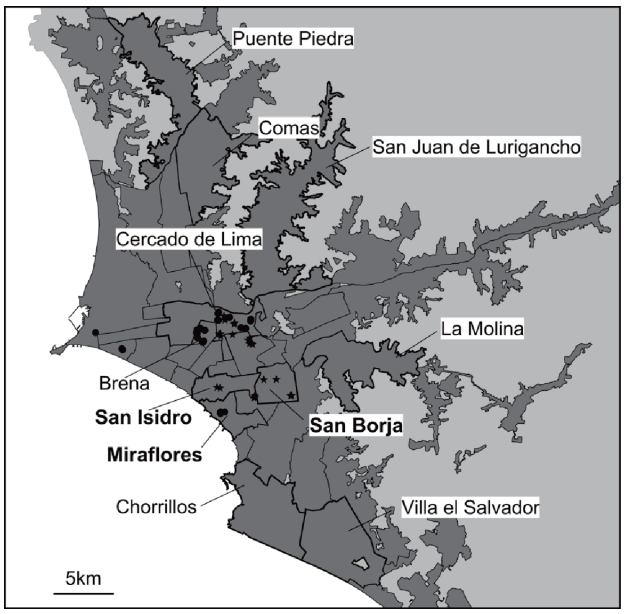

Fig. 2. Lima, Peru, study area. District and detailed field survey sites are indicated.

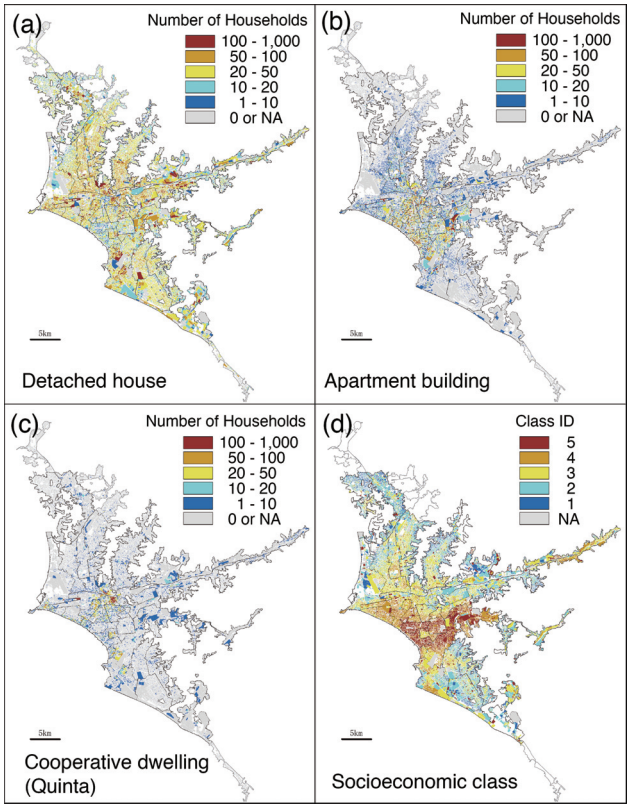

Fig. 3. Distribution of numbers of households by housing use: (a) detached house, (b) apartment building, (c) cooperative dwelling (quinta), (d) distributions of socioeconomic class.

houses account for over 75% of such buildings in the entire city and apartment buildings account for about 15%. **Fig. 3(d)** shows socioeconomic class distribution, with class 5 being the richest. This figure indicates that the rich live in the city center and the poor live in its surroundings.

Wall-construction materials such as adobe, quincha, and masonry/cement brick, which are included in data, show that over 80% of households were in masonry or cement brick buildings. This data is thus used as basic information in creating building inventory data but does not include construction type or building height, which are necessary for estimating earthquake damage.

Building feature data (hereafter, CISMID data) are extracted from field survey conducted by the Japan Peru Center for Earthquake Engineering Research and Disaster Mitigation (CISMID). For gathering the data, CISMID randomly chose 5,200 city blocks – about 30% of the total – from eight districts – Comas, La Molina, Villa el Salvador, Peunte Piedra, San Juan de Lurigancho, Chorrillos, Breña, and Cercado de Lima (**Fig. 2**), and collected data on floor number, usage, construction type, etc., for representative buildings in the target city blocks. The two construction types of representative buildings in these blocks were masonry and concrete, for which masonry accounted for 85%.

Although data contain floor number and construction type, surveyed districts and city blocks were limited, so only part of the city was covered. CISMID data also focused on districts with low earthquake-resistant buildings that could be damaged in an earthquake. An additional survey of about 300 city blocks in districts with mid- and high-rise buildings was therefore conducted in August 2013 and this additional data was included with CISMID data covering the 11 districts shown in **Fig. 2** and 5,500 city blocks.

2.3. Satellite Image and Detailed Local Survey Data

We used digital surface models (DSMs) with observation images taken on October 15, 2008, by the ALOS satellite PRISM sensor and on March 30, 2006, and April 12, 2009, by IKONOS satellite (for details on deriving DSM with data from PRISM, see [7]). Stereoscopic data obtained from stereo-pair sensor images in forward and nadir views and in backward and nadir views were used in the study. For stereoscopic image data obtained in 2006 and 2009 from IKONOS, DSM was created with an analysis module of ERDAS Imagine image processing software. DSM contained both ground evaluation and height data on objects such as buildings and trees, so object height was estimated by data filtering [5]. The maximum object height in each city block was also recorded. Images from the two satellites covered the almost entire Lima area, as shown in **Fig. 4**.

A detailed on-site survey was conducted to examine current conditions of buildings in each city block and the validity of estimation on the number of households, as described in Section 3. In the on-site survey, a video camera with built-in GPS was used to take videos of buildings in each city block from neighboring streets and thereby obtain data on number of stories, households, and usage. Thus, we surveyed 50 city blocks in and near the center of Lima, as indicated by stars and circles in **Fig. 2**.

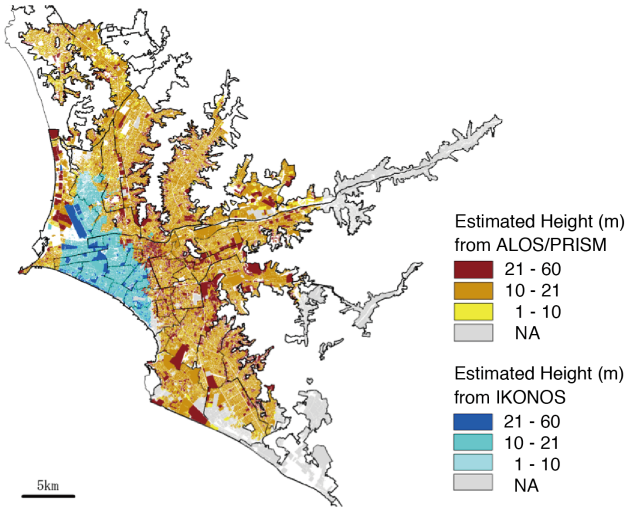

Fig. 4. Distribution of building height information from DSM calculated using ALOS/PRISM and IKONOS images.

3. Development of Lima Building Inventory Data

3.1. Estimation of Number of Households in Building Construction Types

Based on preceding studies [8] and the current state of Peru, seven categories – structural classes – were used as features in building inventory that were suitable for the estimating earthquake damage. As shown in **Fig. 5**, these were derived from the housing use type, wall-materials, and socioeconomic classes in census data:

- A: Adobe, etc., low-rise, 1-2 stories
- M1: Nonengineered masonry, low-rise, 1-2 stories
- M2: Reinforced or confined masonry with flexible slabs, low-rise, 1-2 stories
- M3: Reinforced or confined masonry with rigid slabs, low-rise, 1-2 stories
- M4: Reinforced or confined masonry with rigid slabs, mid-rise, 3-6 stories
- M5: Reinforced concrete frames, mid-rise, 3-6 stories
- M6: Reinforced concrete frames, high-rise, 7 or more stories

Socioeconomic classes of residents and building construction types are correlated [9]. Based on the relation between socioeconomic classes in census data and representative construction types and number of stories in CISMID data, the percentage of each building construction type in each area was calculated for different socioeconomic classes. **Table 1** shows the relation between socioeconomic classes and building construction types of detached houses and quinta. M1 buildings account for 25% and M2 for 45% in the class 1 area, where many low-income residents live. In the class 5 area, where many high-income residents live, there are no buildings of these types and almost all buildings are M3. The numbers of

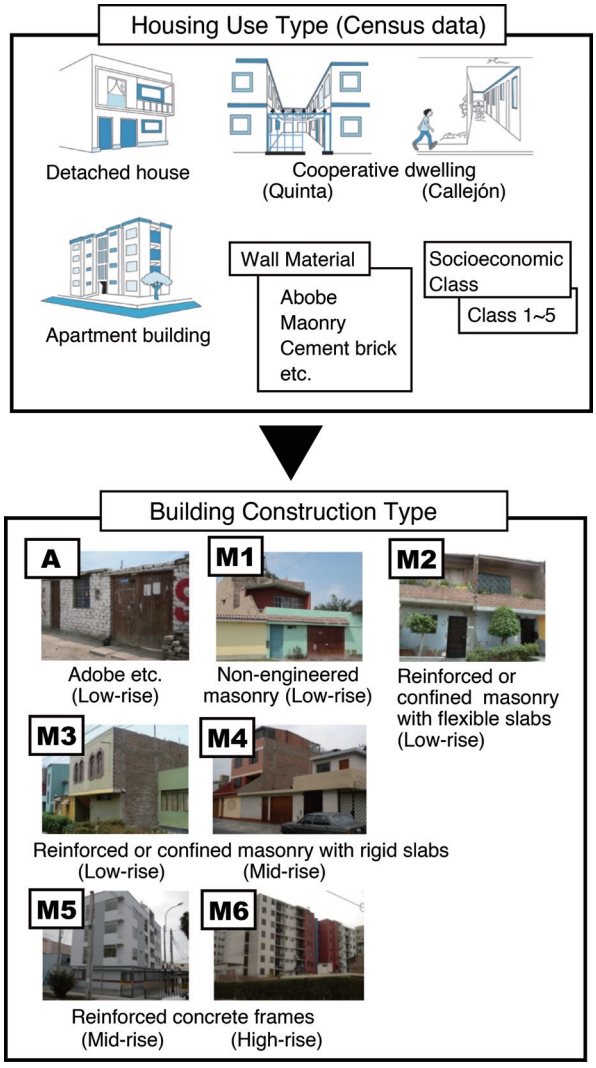

Fig. 5. Building construction type estimation based on housing use with wall material and socioeconomic class in census data.

households in detached houses and in quinta are known in census data and multiplied based on percentages to calculate the number of households of each building construction type.

Table 2 shows the relation between socioeconomic class and apartment building. For analysis, city blocks were divided to those with only mid- or low-rise buildings (**Table 2(a)**) and those also including high-rise buildings (**Table 2(b)**). The increase in the number of households in buildings with different number of stories obtained in the detailed field survey was taken into account. It was found from analysis that socioeconomic classes and building construction types correlated mutually and that in areas where high socioeconomic class residents lived, dwellers tended to live in high-rise buildings with relatively high-earthquake resistance. In the socioeconomic class 5 area with many tall buildings, 75% of households were in M6 buildings.

Based on the above preliminary study, we constructed a flowchart of conversion to building construction type (A, M1-M6) and an estimation of the number of households, given in **Fig. 6**, explained below.

Table 1. Distribution ratio of building construction type by socioeconomic class (detached house and quinta).

Socioeconomic class	Distribution ratio (%)		
	M1	M2	M3
Class-1	25	45	30
Class-2	15	25	60
Class-3	15	10	75
Class-4	5	0	95
Class-5	0	0	100

Table 2. Distribution ratio of households in each building construction type by socioeconomic class (apartment building).

(a) City block with low- and mid-rise building.

Socioeconomic class	Distribution ratio (%)		
	M3	M4	M5
Class-1	100	0	0
Class-2	40	60	0
Class-3	5	95	0
Class-4	0	85	15
Class-5	0	65	35

(b) City block including high-rise building.

Socioeconomic class	Distribution ratio (%)			
	M3	M4	M5	M6
Class-1	100	0	0	0
Class-2	40	60	0	0
Class-3	10	55	10	25
Class-4	0	30	30	40
Class-5	0	5	20	75

1) Based on the data of wall materials in census data, the number of households in city blocks was divided into those in adobe buildings and those in masonry or cement brick buildings. The number of households living in adobe buildings was used as the number of households living in type A buildings.

2) The number of households living in masonry or cement brick buildings was first divided into those in detached houses, those in apartment buildings, those in callejón, and those in quinta, based on housing use type data in census data.

3) The number of households in M1 type buildings was calculated assuming that 80% and 20% of callejón buildings are type A and M1, respectively.

4) It is assumed that detached houses and quinta were type A or M1-M3 buildings. The number of households in type A calculated above and the number of households in M1 among callejón were subtracted from the number of households in detached houses,

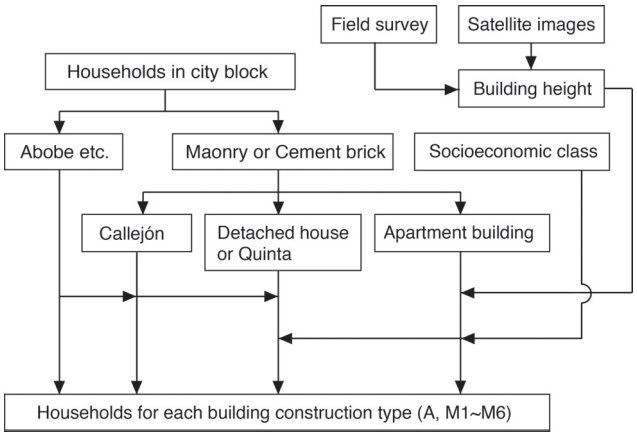

Fig. 6. Estimation flowchart for number of households by building construction type using census data, satellite images, and field survey results.

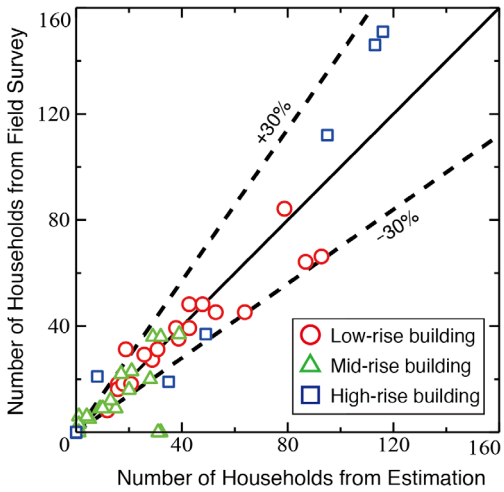

Fig. 7. Estimated household number versus actual number observed in a field survey.

quinta, and callejón. This was done to calculate the total number of households in detached houses and quinta. Next, the ratio of buildings of each construction type and socioeconomic class was multiplied by the number of households in detached houses and quinta to classify households in detached houses and quinta into those living in M1, M2, or M3 buildings.

5) Apartment buildings consist of M3-M6, these building construction types should be classified by height. Object height data on city blocks obtained from DSM were used to classify city blocks into those with only low- and mid-rise buildings and those also including high-rise buildings. By comparing the data of number of stories from the detailed field survey and object height data, we defined high-rise buildings as those 21 m or higher. Next, the number of households in city blocks with only low- and mid-rise buildings was divided to households in M3 to M5 buildings taking into account the distribution ratio of buildings of each type classified by socioeconomic class, as shown in **Table 2(a)**. The number of households in city blocks that also included high-rise buildings was divided into those of households in M3 to M6 using the ratio in **Table 2(b)**.

6) The numbers of households in A and M1 through M6 buildings were determined by summing the number of households in buildings of each construction type.

3.2. Validation of Estimation and its Application to the Entire Lima City Area

Based on the above procedure, the number of households for different building construction types was estimated and examined in terms of estimation precision for city blocks where the field survey was conducted. Since no detailed building construction type data were obtained in the survey, the numbers of households in building types A and M1-M6 cannot be confirmed. The estimated number of households in low-, mid-, and high-rise buildings was compared to the actual number of households in the field survey. Results are shown in **Fig. 7**, in which the number of households was estimated to within error of 30% or less.

The proposed procedure to estimate the number of households in each building construction type was applied to 75,000 Lima blocks. **Fig. 8** shows the distribution of the number of households for different building construction types. Type A buildings are concentrated in the oldest part of city and types M1 and M2 distributed widely outside of the city center. The number of households in M3 buildings is highest. The number in M4 buildings is also high but rather concentrated at the city center. Residents of types M5 and M6 are more concentrated at the city center. **Fig. 9(a)** shows the distribution of the number of households in each district. **Fig. 9(b)** shows the ratio of households in buildings with low-earthquake resistance, i.e. the number of households in A, M1, and M2 buildings divided by the total number of households in the district. The total number of Lima households is about 1.84 million and residents of buildings with low-earthquake resistance are located in the Lima suburbs.

4. Estimating Earthquake Damage for Lima

4.1. Fragility Curves for Different Building Construction Types

As shown in **Fig. 1**, damage occurrence probability for different building construction types must be calculated to estimate earthquake damage. This calculation requires fragility curves for different building construction types. Peru essentially has no appropriate, easy-to-use fragility curves for the building construction types suitable for this study. Although knowledge and opinions could be collected from specialists using the Delphi method to obtain seismic performance of buildings and apply them to estimating earthquake damage [10], we instead used damage fragility curves proposed in previous studies.

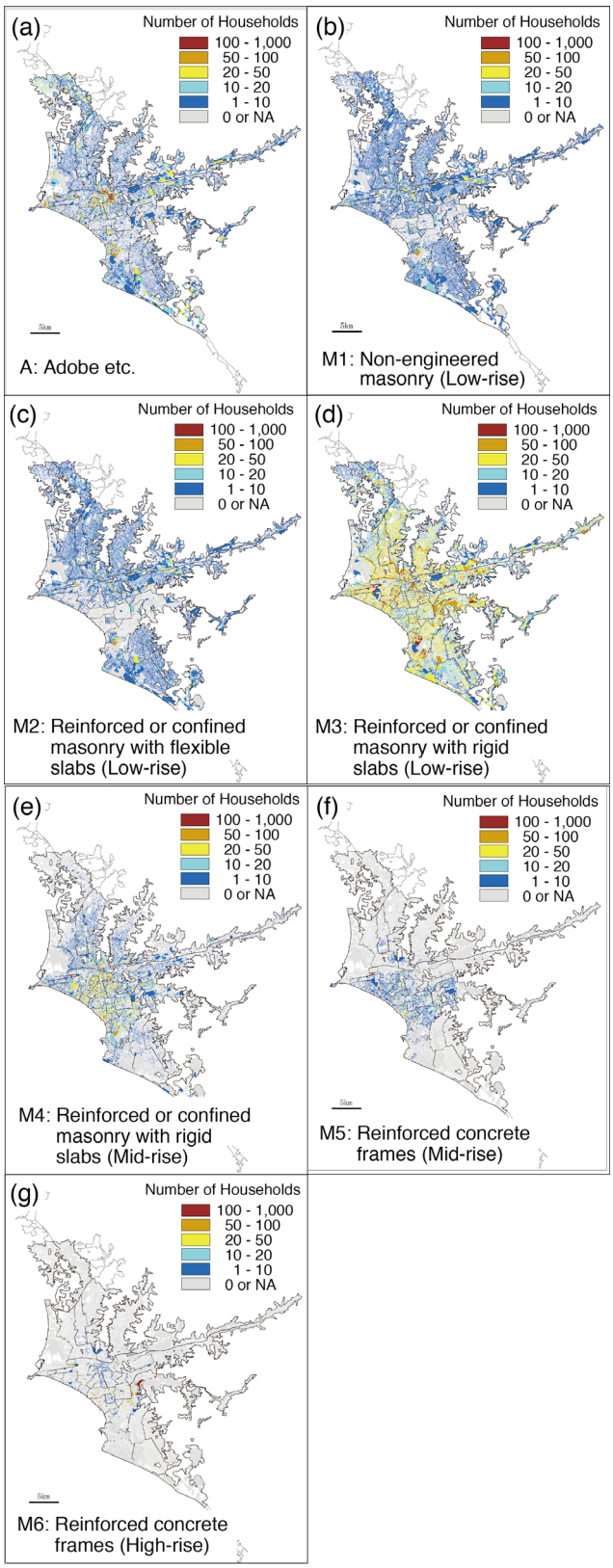

Fig. 8. Distribution of estimated number of households by building construction type: (a) adobe, etc., (b) nonengineered masonry (low-rise), (c) reinforced or confined masonry with flexible slabs (low-rise), (d) reinforced or confined masonry with rigid slabs (low-rise), (e) reinforced or confined masonry with rigid slabs (mid-rise), (f) reinforced concrete frames (mid-rise), (g) reinforced concrete frames (high-rise).

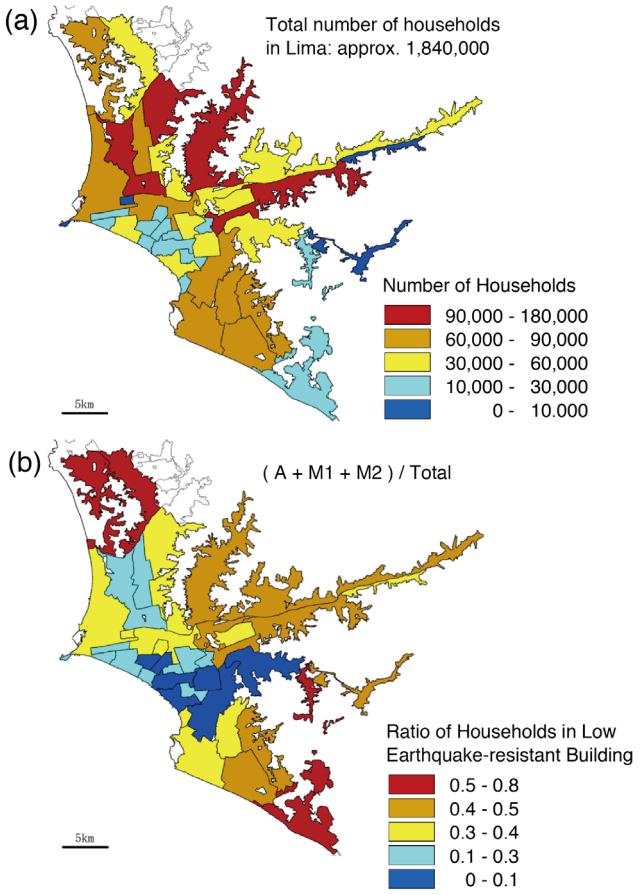

Fig. 9. Distribution of estimated number of households for each district: (a) total number of households, (b) ratio of household in low earthquake-resistant buildings.

Matsuzaki et al. (2013) created fragility curves of seriously damage which corresponds with Grade 4 or 5 in damage scale of EMS-98 [11] for adobe and masonry buildings based on the results of the building damage survey in Pisco caused by the 2007 Pisco earthquake and peak ground acceleration (PGA) of ground motion obtained in numerical simulation [12]. Adobe buildings in Pisco would be similar to adobe buildings in Lima. Matsuzaki et al. also mentioned that masonry buildings were reinforced with RC columns and beams [12] that correspond to M3 and M4 masonry buildings in this study. No detailed damage fragility curves were available for distinguishing M3 and M4 in the study by Matsuzaki et al. (2013) or in other previous studies, so we used fragility curves given by Matsuzaki et al. (2013) for A and M3&M4.

No fragility curves were available, either, for buildings of nonengineered masonry (M1) or low earthquake-resistant masonry (M2). Assuming that M1 and M2 had the same quake resistance, we created a fragility curve for M1&M2 to place it between A and M3&M4 obtained by Matsuzaki et al. (2013), as shown in **Fig. 10**.

Quiroz and Maruyama (2014) created a reinforced concrete model for 10-story RC buildings in Lima based on vibration experiments and derived fragility curves as a function of PGA for RC buildings using simulated quake

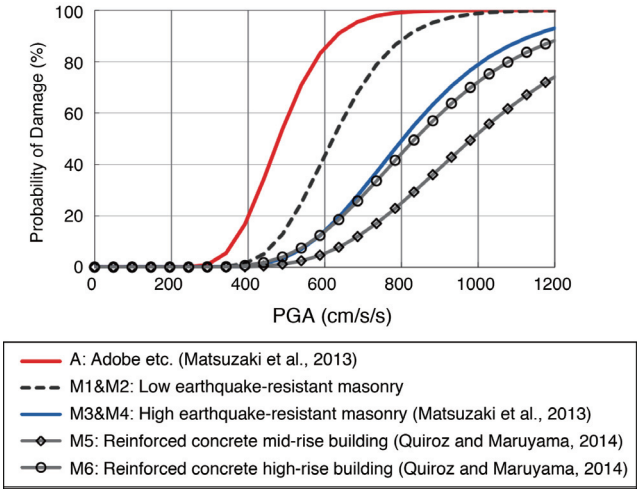

Fig. 10. Fragility curves by building construction type.

motion [13]. This study used the results to obtain the fragility curves for M5 and M6 (**Fig. 10**). It is found that damage to type A and other low earthquake-resistant buildings begins occurring at a small PGA and curves are steeper than those of M5 and M6. This indicates that larger earthquake ground motion would dramatically increase the number of damaged buildings.

4.2. Estimation of Damage Due to Anticipated Future Earthquake

In its location near the boundary between the South American and Nasca tectonic plates, Peru has many earthquakes. Pulido et al. (2014) estimated the focal area of an anticipated great fault earthquakes of Mw8.9 based on geodetic data from earthquakes occurring in Peru since 1746 [14]. They calculated the distributions of peak ground acceleration (PGA) for 108 scenarios for the combination of 12 focal areas and 9 destruction start points, and estimated the average and standard deviation among these scenarios. In this study, the average PGA in 108 scenarios and the average plus one standard deviation were both used as input ground motion parameters. **Fig. 11** shows the distributions. Ground motion is large near coastal areas and the value of average plus one standard deviation exceeded 1,000 cm/s/s in some places.

For about 75,000 city blocks in Lima, damage probability was obtained from fragility curves (**Fig. 10**) based on input PGA and multiplied by the number of households in building inventory data in Section 3 to calculate the number of households that would be seriously damaged based on different building construction type. **Fig. 12** shows the number of households that would be seriously damaged in different districts. When input PGA is the average value, about 48,000 households would be seriously damaged. In contrast, for the average plus one standard deviation, the number would increase dramatically to about 430,000.

For the case in which input PGA is set to average plus one standard deviation, **Fig. 13** shows the ratio of number of households that would be seriously damaged in individual districts divided by the number of households in the district. Results show that districts near the coastal area would tend to have a higher rate serious damage because input PGA is relatively higher in these districts. In areas with many buildings having low earthquake resistance (**Fig. 9(b)**), damage was severe even if input PGA was small because damage probability rapidly increases within a PGA range from 400 to 600 cm/s/s, as shown by fragility curves for A and M1&M2 buildings in **Fig. 10**. In Lima, about 70% of households in seriously damaged buildings are caused from low earthquake-resistant buildings (A+M1+M2).

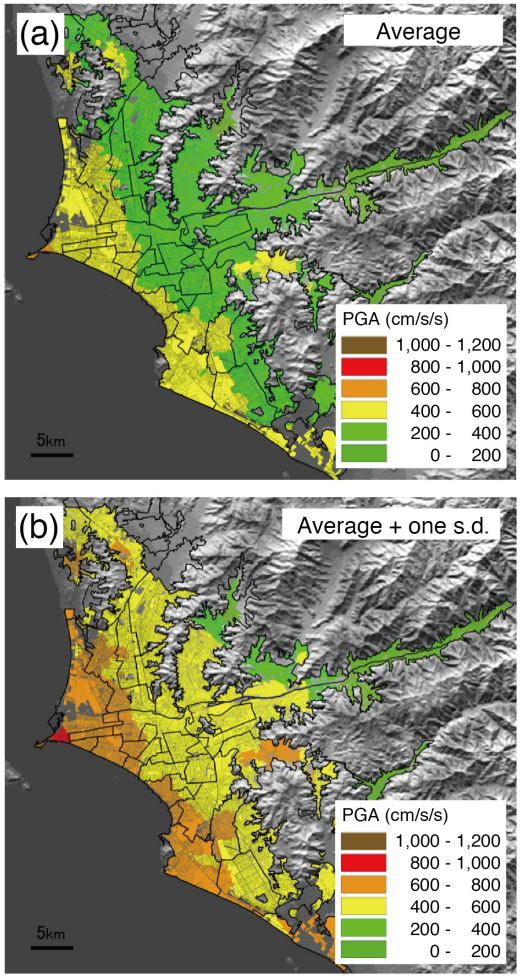

Fig. 11. Distribution of peak ground velocity (PGA) for earthquake scenarios: (a) average value calculated from 108 scenario earthquakes, (b) average + one standard deviation calculated from 108 scenario earthquakes.

In order to evaluate the effect of earthquake retrofitting in Lima city, two retrofitting cases were considered. Since A and M1&M2 buildings were likely to be severely damaged, Case 1 was a case in which A buildings were renovated into a M1 or M2 level and Case 2 was a case in which A, M1, and M2 buildings were all renovated into a highly earthquake-resistant masonry of M3 or M4. **Fig. 14** shows the number of households in buildings that would likely be seriously damaged in Case 1, and **Fig. 15** shows that for Case 2. Both figures show results for aver-

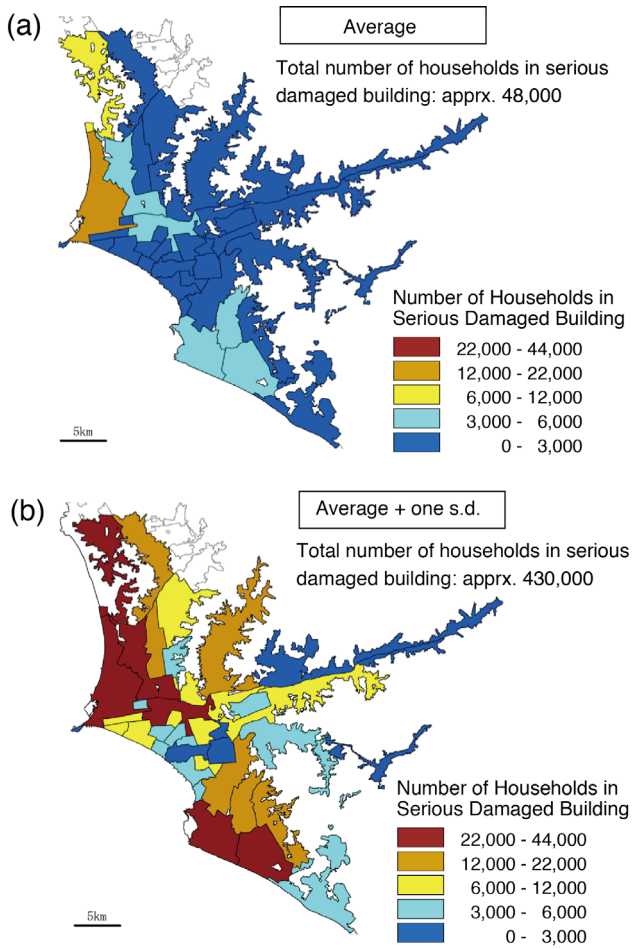

Fig. 12. Distribution of estimated number of households in serious damaged buildings by district for earthquake scenarios: (a) average value calculated from 108 earthquake scenarios, (b) average + one standard deviation calculated from 108 earthquake scenarios.

age and for average plus one standard deviation as input PGA. Case 1 reduced the number of households in buildings that would be seriously damaged to about 14,000, or about 71%. When input PGA was large – the average plus one standard deviation – reduction was about 23%. In contrast, Case 2 reduced the number of households in buildings that would be seriously damaged to about 200,000 and reduction of over 50% when input PGA was large – average plus one standard deviation. Seismic retrofitting in Lima city was thus found to be effective in reducing earthquake damage.

5. Conclusions

For estimating earthquake damage in developing countries and areas where building inventory data are not available, we have proposed a simple method for generating building inventory data using GIS data from census, satellite imagery, and data from field surveys. The entire city area of Lima, Peru, which faces high seismic risk similar to that in Japan, was chosen as our research target.

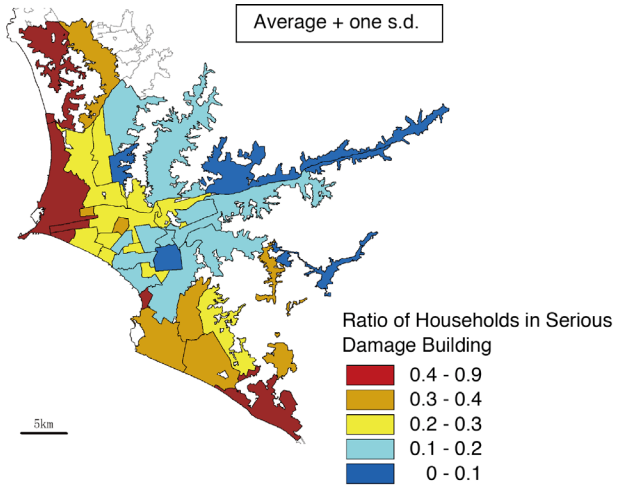

Fig. 13. Distribution of ratio of households in seriously damaged buildings by district.

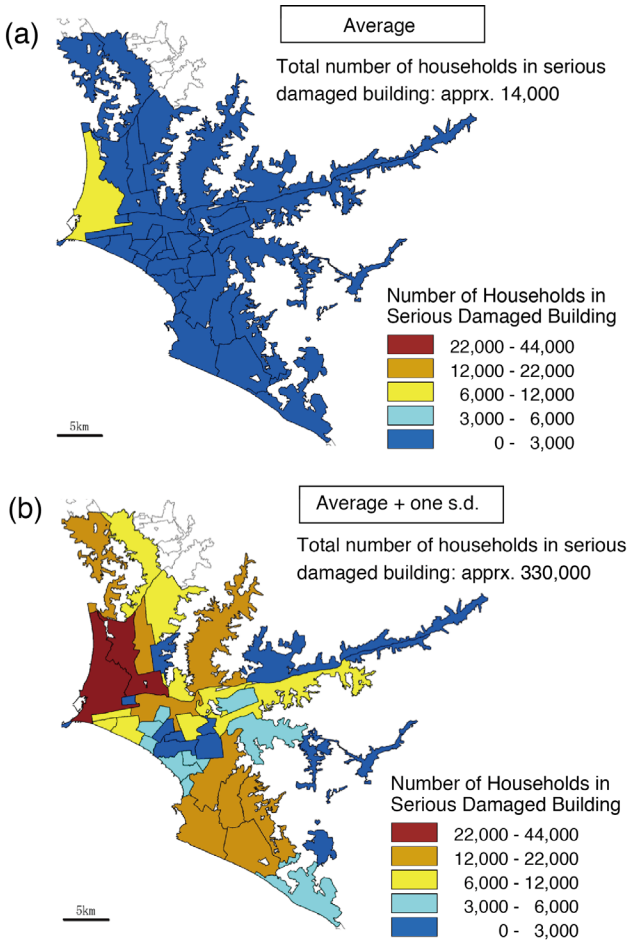

Fig. 14. Distribution of estimated number of households (retrofit Case 1) in serious damaged buildings by district for earthquake scenarios: (a) average value calculated from 108 scenario earthquakes, (b) average + one standard deviation calculated from 108 scenario earthquakes.

Based on housing use type, wall material, and socioeconomic class in census data and object height information from satellite images, the classification procedure of

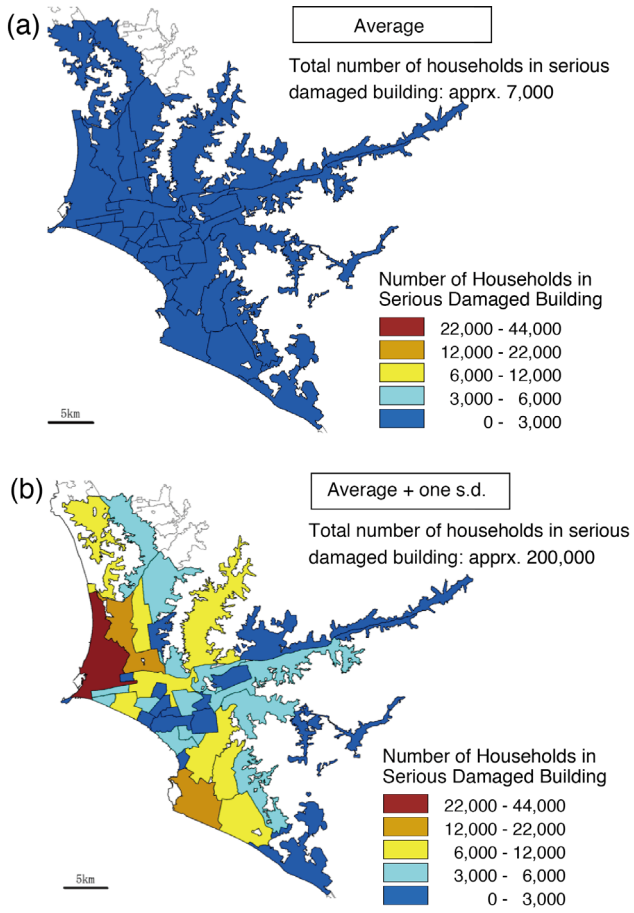

Fig. 15. Distribution of estimated number of households (retrofit Case 2) in serious damaged buildings by each district for earthquake scenarios: (a) average value calculated from 108 earthquake scenarios, (b) average + one standard deviation calculated from 108 earthquake scenarios.

building construction types taking into account their seismic fragility. Building inventory data for all of Lima were determined using this procedure and estimation accuracy was evaluated by comparing data for city blocks where the detailed field survey was conducted. It was found that the number of households was estimated with about 30% precision.

By calculating the damage probability of buildings based on fragility curves for the input ground motion of an anticipated earthquake and multiplying probability by created building inventory data, we estimated the number and distribution of households in buildings that could be seriously damaged. Results showed that the risk of damage was higher in districts close to the coastal area and districts containing many low earthquake-resistant buildings. The feasibility of seismic retrofitting was verified and it was also shown that the number of households in buildings that would be seriously damaged could be reduced by half if adobe and low earthquake-resistant masonry buildings could be renovated into high earthquake-resistant buildings such as reinforced or confined masonry with rigid slabs.

Acknowledgements

PRISM images from ALOS satellite are owned by the Japan Aerospace Exploration Agency. IKONOS images are owned by GeoEye. These images and DSM data were provided by the Remote Sensing Technology Center of Japan. We thank the graduates of the Tokyo Institute of Technology, Mr. Takeshi Takase, Mr. Yusuke Hirano, and Mr. Kota Araki for data analysis, and Dr. Jenny Taira and Mr. Jorge Morales from CISMID for support in the field survey. This study was supported in part by a Science and Technology Research Partnership for Sustainable Development (SATREPS) project, titled "Enhancement of Earthquake and Tsunami Disaster Mitigation Technology in Peru (Principal Investigator: Prof. Fumio Yamazaki)."

References:

[1] K. Hasegawa and S. Midorikawa, "Seismic Risk Mapping of Wooden House in Large Area Using the Grid-square Statistics: Part 1 Estimation of population of wooden houses with different construction age," Journal of Structural and Construction Engineering, Architectural Institute of Japan, No.497, pp. 75-80, 1997 (in Japanese with English abstract).

[2] K. Hasegawa and S. Midorikawa, "Seismic Risk Mapping of Non-wooden Building in Large Area Using the Grid-square Statistics," Journal of Structural and Construction Engineering, Architectural Institute of Japan, No.521, pp. 41-47, 1999 (in Japanese with English abstract).

[3] H. Miura and S. Midorikawa, "Updating GIS Building Inventory Data Using High-resolution Satellite Images for Earthquake Damage Assessment: Application to Metro Manila, Philippines," Earthquake Spectra, Vol.22, No.1, pp. 151-168, 2006.

[4] I. F. Shaker, A. Abd-Elrahman, A. K. Abdel-Gawad, and M. A. Sherief, "Building Extraction from High Resolution Space Images in High Density Residential Areas in the Great Cairo Region," Remote Sensing, Vol.3, No.4, pp. 781-791, 2011.

[5] M. Matsuoka, H. Miura, S. Midorikawa, and M. Estrada, "Extraction of Urban Information for Seismic Hazard and Risk Assessment in Lima, Peru Using Satellite Imagery," Journal of Disaster Research, Vol.8, No.2, pp. 328-345, 2013.

[6] Instituto Nacional de Estadistica e Informatica (INEI): National Census 2007: Population XI and VI Housing, http://www.inei.gob.pe/estadisticas/censos/ [access available on Jul.1, 2014]

[7] J. Takaku and T. Tadano, "PRISM On-Orbit Geometric Calibration and DSM Performance," IEEE Transaction on Geoscience and Remote Sensing, Vol.47, No.12, pp. 4060-4073, 2009.

[8] Federal Emergency Management Agency (FEMA): HAZUS®MH MR4 Earthquake Model Technical Manual, Washington D.C., 2009.

[9] C. Zavala, M. Estrada, F Lazares, S. Alarcon, J. Taira, and J. Morales, "Quick Risk Evaluation of Earthquake Losses on Housing," Proc. Of 15th World Conference on Earthquake Engineering, ID: 3779, p. 9, 2012.

[10] H. Miura, S. Midorikawa, K. Fujimoto, B. M. Pacheco, and H. Yamanaka, "Earthquake Damage Estimation in Metro Manila, Philippines based on Seismic Performance of Buildings Evaluated by Local Experts' Judgments," Soil Dynamics and Earthquake Engineering, Vol.28, pp. 764-777, 2008.

[11] B. Grunthal, "European Macroseismic Scale 1998," European Seismological Commission, 1998.

[12] S. Matsuzaki, N. Pulido, H. Yamanaka, K. Chimoto, Y. Maruyama, and F. Yamazaki, "Vulnerability Estimation of Building Using Damage Survey Data Following the 2007 Pisco, Peru Earthquake," Journal of Social Safety Science, No.21, pp. 27-36, 2013 (in Japanese with English abstract).

[13] L. G. Quiroz and Y. Maruyama, "Assessment of performance of Peruvian high-rise thin RC wall buildings using numerical fragility functions," Proceedings of the 2014 World Congress on Advances in Civil, Environmental, & Material Research (ACEM14), Paper No. M4F.3.CC406_728F, 2014.

[14] N. Pulido, Z. Aguilar, H. Tavera, M. Chlieh, D. Calderón, T. Sekiguchi, S. Nakai, and F. Yamazaki, "Source Models Scenarios and Strong Ground Motion for Future Mega-earthquakes: Application to Lima, Central Peru," Bulletin of Seismological Society of America, 2014 (in press).

Name:
Masashi Matsuoka

Affiliation:
Associate Professor, Department of Built Environment, Tokyo Institute of Technology

Address:
4259-G3-2, Nagatsuta, Midori-ku, Yokohama 226-8502, Japan

Brief Career:
1992 Research Associate, Tokyo Institute of Technology
1996 Engineer, Remote Sensing Technology of Japan
1998 Deputy Team Leader, RIKEN
2004 Team Leader, National Research Institute for Earth Science and Disaster Prevention
2007 Senior Research Scientist, National Institute of Advanced Industrial Science Technology
2010 Division Chief, National Institute of Advanced Industrial Science Technology
2012- Associate Professor, Tokyo Institute of Technology

Selected Publications:
• Matsuoka and Yamazaki, "Use of Satellite SAR Intensity Imagery for Detecting Building Areas Damaged due to Earthquakes," Earthquake Spectra, EERI, Vol.20, No.3, pp. 975-994, 2004.
• Matsuoka and Nojima, "Building Damage Estimation by Integration of Seismic Intensity Information and Satellite L-band SAR Imagery," Remote Sensing, MDPI, Vol.2, No.9, pp. 2111-2126, 2010.
• Matsuoka and Yamazaki, "Comparative Analysis for Detecting Areas with Building Damage from Several Destructive Earthquakes Using Satellite Synthetic Aperture Radar Images," Journal of Applied Remote Sensing, SPIE, Vol.4, 041867, 2010.

Academic Societies & Scientific Organizations:
• Earthquake Engineering Research Institute (EERI)
• Architectural Institute of Japan (AIJ)
• Remote Sensing Society of Japan (RSSJ)